FEBRUARY
1965

ROYAL AIRCRAFT ESTABLISHMENT

TECHNICAL REPORT No. 65031

CALCULATION OF OPTICAL TRANSFER FUNCTIONS FROM LENS DESIGN DATA

by

A. C. Marchant

Margaret Lello

MINISTRY OF AVIATION
FARNBOROUGH HANTS

U.D.C. No. 535.316/317

ROYAL AIRCRAFT ESTABLISHMENT

Technical Report No.65031

February 1965

CALCULATION OF OPTICAL TRANSFER FUNCTIONS FROM LENS DESIGN DATA

by

A. C. Marchant

Margaret Lello

SUMMARY

This Report describes the basic theory and the method of operation of a computer programme developed at Imperial College, London, for calculating the optical transfer function of a lens system. The programme determines the wave-front aberration, and the shape of the exit pupil (vignetted or otherwise) and uses this information to derive the transfer function in any image plane and at any field angle. Typical results, for a modern aerial reconnaissance lens, are given and compared with measurement.

Departmental Reference: IEE 80

CONTENTS

1 INTRODUCTION

The merits of the optical transfer function as a means of assessing lens performance are now well established[1,2].

By analogy with other communication processes, an optical system is regarded as a low-pass, linear filter whose characteristics can be specified by means of transfer, or frequency response, curves showing the variation of amplitude and phase of a transmitted signal with its spatial frequency. In the present context, the "signal" is represented by a two-dimensional grating-like object consisting of infinitely long parallel lines, the light intensity varying sinusoidally between one line and the next. The "amplitude" is half the difference of intensity between brightest and darkest parts of the pattern (Fig.1). "Phase" denotes a lateral displacement of the lines in a direction perpendicular to their length, and is expressed as the ratio of this displacement to the line separation.

"Frequency" is the reciprocal of this separation, usually quoted as the number of lines per millimeter.

To accord with visual impressions, amplitude is usually related to "contrast" which is itself defined as the ratio of amplitude to mean intensity. If I_{max} and I_{min} represent maximum and minimum intensities in the pattern, then

$$\text{Contrast} = \frac{(I_{max} - I_{min})/2}{(I_{max} + I_{min})/2} = \frac{I_{max} - I_{min}}{I_{max} + I_{min}} .$$

A plot of contrast and phase against spatial frequency (see Fig.16) gives complete information about the image-forming properties of a lens system, and allows a precise assessment to be made of its performance when used with any given image receiver or sensor. Recent advances in diffraction theory make it possible to calculate transfer curves from lens design data, so that it is now practicable to investigate which of a number of available designs will meet a given functional specification without having to manufacture a prototype lens and test its performance under the actual conditions of use.

This Report describes the main features of a computer programme, (recently developed under Ministry of Aviation sponsorship by the Imperial College of Science and Technology) the method of operation, and finally gives some examples of the results obtained.

2 THEORY OF IMAGE FORMATION

2.1 Fundamentals

The theory underlying this method of calculating optical transfer functions is based essentially on Abbe's theory of image formation[3].

As these ideas are not generally familiar, it is worthwhile to outline them briefly before describing their extension in the present work.

Abbe was primarily concerned with imagery in the microscope. Fig.2 illustrates the conditions obtaining with so-called "Köhler" illumination of the object G, in which light from each point of the source s is rendered parallel by the condenser c before passing through the object. For simplicity we will assume initially that the source is very small, and that the object is a simple grating of opaque sharp-edged lines and clear spaces. The parallel beam passing through the grating then gives rise to a Fraunhofer diffraction pattern behind the microscope objective M. This pattern consists of a number of secondary images of the source; ray paths to two of these (-1 and 1) are shown in the figure and others are indicated by 2, 3, 4 etc.

Now according to Abbe the image of the grating, formed in the plane G', can be thought of as an interference pattern formed by the light from all these secondary (coherent) sources.

Thus the pair 1 and -1 acting alone would give a pattern of interference fringes, in which the light intensity varies co-sinusoidally with distance from the axis GG', the separation of the fringes being dependent on the separation of the two sources and on the distance OG'.

Similarly, the pair 2 and -2 acting alone, would give a fringe separation of half that in the previous case, 3 and -3 would give still more closely spaced fringes, and so on.

The final image is the combination of all these separate interference patterns with the uniform illumination provided by the central source O, and is a perfect reproduction of the object provided the objective is free from aberration and accepts all the diffracted light from the grating. This can in actual practice never be the case (because the objective would require to be of infinite aperture) so that the image is always degraded. If the aperture of the objective is reduced so far that only the light contributing to "sources" -1, 0 and 1 is accepted, then the final "image" is a nearly sinusoidal fringe pattern, instead of the sharp-edged pattern required, although the fringe spacing is the same as the bar spacing would be in the ideal image.

2.2 "Sine wave" objects

At this point it is necessary to define more precisely what is meant by the "sinusoidal" grating object referred to in Section 1. The simple fringe pattern which represents the image of such an object can be produced by only two diffraction maxima, equally spaced each side of the optical axis.

The amplitude A(x) of the wavefront, immediately after transmission through the grating, varies with distance x (measured perpendicular to the bars) across it in the following way:-

$$A(x) = A_o \cos\left(\frac{\pi x}{L}\right) \qquad (2.1)$$

where A_o is a constant, and L the distance between neighbouring bars, or the spatial "wavelength".

Equation (2.1) defines the optical "signal" with which we shall be concerned in this Report.

Because of the negative values of amplitude associated with this expression, and the absence of a central order in the diffraction pattern, such a grating would have the physical form illustrated in Fig.3. The transmission varies continuously from zero at the centre of a bar to a maximum at the centre of the adjacent space, and each alternate bar is covered by a transparent phase-changing strip which produces a retardation of π in the phase of the light passing through it. The three right-hand drawings show respectively the shape and the variation of amplitude and intensity of the wavefront leaving the grating.

2.3 Incoherent illumination

The discussion so far has been restricted to coherent illumination of the object, that is to say it is assumed that a fixed phase relationship exists between wave elements emerging from different parts of the grating. This implies that a single radiating source is involved. The more general case of incoherent illumination is represented by an infinite extension of the light source s in all directions, in a plane indicated by the dotted line in Fig.2. An infinite number of independently radiating sources are now present, each one providing a parallel beam through the grating. One such beam is illustrated by the chained lines in Fig.2. With the sinusoidal object defined in the previous section, each beam provides a pair of diffraction maxima, and the final image is the sum of all the separate fringe patterns, each of which arises from one pair of maxima.

Fig.4(a) shows a view of the aperture of the microscope objective as seen from G'. Suppose the spatial frequency of the grating is such that the maxima it produces are spaced by a distance s. Two such maxima are indicated by the points AA in Fig.4(a). An infinite number of other pairs with separation s will be present in the aperture, but will be confined to the two shaded areas, because the companion to any maximum which lies outside these areas will not fall within the lens aperture and will not therefore contribute to the interference patterns in the image plane.

The points BB in the figure represent such a "forbidden" pair.

2.4 Effects of lens aberration

The point has now been reached at which it is necessary to consider how the final distribution of intensity in the image plane depends on the diffraction pattern behind the objective, or in what is strictly the exit pupil of the system shown in Fig.2. If all the secondary sources radiate with the same phase in a spherical surface centred at the image point G', there will be a maximum of intensity at this point since by Huygen's principle the wave elements emitted from each source pair in the surface have equal distances to travel and will interfere constructively. The total effect at G' is found by summing the intensities of all the separate interference patterns, and the image of a "bright bar" of the original grating appears at this point.

Exactly the same conditions apply at other points in the neighbourhood of G' at which other bright lines of the grating are imaged. (It should be emphasised that in this theory one is concerned essentially with very small scale effects, and with areas of the image plane which are very small compared to their distance from the exit pupil of the optical system.)

If the lens system introduces aberration, the phases of the diffraction maxima are no longer equal in the spherical reference surface, and complete constructive interference does not occur at G' and similar points. The general effect is that the "contrast" (see Section 1) of the image is reduced and there may also be a slight lateral movement, or "phase shift" of the lines.

As will be shown later, it is possible, given the wavefront aberration of the lens system, and consequently the relative phases of the diffraction maxima in the exit pupil, to calculate the contrast and phase of the image accurately.

2.5 General application of the theory

Although Abbe's theory was originally applied to the microscope, the same ideas can readily be extended to any other type of optical system.

For example, with the photographic lens the object would be nominally at infinity. The light leaving it would normally be incoherent and the object could be simulated by a transparent grating with a large "effective source" (previously represented by the plane s and condenser c in Fig.2) behind it.

The diffraction maxima are formed in the entrance pupil of the lens system, now infinitely distant from the grating. They are then imaged through to the exit pupil with phase variations imposed, due to the aberrations of the lens system, and the final image is formed by interference in the focal plane.

3 BASIC FORMULAE

A simplified derivation of the fundamental formulae will now be given: for a more rigorous treatment the work of Hopkins[4] should be consulted. The aim here is primarily to illustrate the physical principles involved.

Consider the interference of waves from a pair of maxima AA, separation s (Fig.5) formed by a simple sine wave grating.

Let the phases of these maxima, in the spherical reference surface centred at G' and passing through the centre E of the exit pupil, be represented by $\phi_{x,y}$ and $\phi_{x-s,y}$.

Then the complex amplitude at a point P of the image plane in the neighbourhood of G' is given by:-

$$\delta A(u,v) = e^{i\phi_{x,y}}\, e^{i(ux+vy)} + e^{i\phi_{x-s,y}}\, e^{i[u(x-s)+vy]}$$

(see Appendix)

where u and v are the coordinates of P.

To find the resulting intensity at P, the above expression is multiplied by its complex conjugate, giving

$$\delta I(u,v) = \{2 + 2\cos(us - [\phi_{x,y} - \phi_{x-s,y}])\} \quad .$$

The intensity therefore varies sinusoidally with distance u across the image plane, reaching a maximum value of 4 and a minimum value of zero. The contrast, by the definition of Section 1, is therefore unity and is independent of the separation s of the sources. Since this separation depends on the line-spacing in the object and also controls the line-spacing in the image, it follows that the contrast in the image is independent of spatial frequency, when only a single source-pair is involved (coherent light). The position of the lines in the

image plane, however, depends on the phase term $[\phi_{x,y} - \phi_{x-s,y}]$ and this will vary according to the position of the source-pair in the exit-pupil.

For a single spatial frequency and incoherent illumination, therefore, an infinite number of sinusoidal patterns, all of the same contrast, appear in the image plane, the peaks of one pattern being slightly displaced from those of another. The resultant effect is found by summing the intensities of all the patterns at each point in the image plane. Hence

$$I_S(u,v) = 2 \iint_S \{1 + \cos(us - [\phi_{x,y} - \phi_{x-s,y}])\} \, dx \, dy \quad .$$

The integral is taken over the area S of the exit pupil within which the effective source-pairs lie (See Fig.4), each source effectively covering an elementary area dx dy of the exit pupil. To this expression must be added the contribution of single sources covering the "forbidden" area of the exit pupil (unshaded area in Fig.4) which can be written as

$$I(u,v)_{A-S} = 2 \iint_{A-S} dx \, dy$$

where A denotes the whole area of the exit pupil.

Expanding the cosine in the previous expression then gives

$$I(u,v) = 2 \iint_A dx \, dy + 2 \cos(us) \iint_S \cos[\phi_{x,y} - \phi_{x-s,y}] \, dx \, dy$$

$$+ 2 \sin(us) \iint_S \sin[\phi_{x,y} - \phi_{x-s,y}] \, dx \, dy$$

when terms which are invariant with x and y are taken outside the integral, and the "single source" term has been added.

The last equation again represents a sinusoidal distribution of the form

$$I(u,v) = C + D \cos(us - \Phi) \qquad (3.1)$$

in which C denotes the term $2 \iint_A dx \, dy$ and

$$D = 2\sqrt{\left[\iint_S \cos(\phi_{x,y} - \phi_{x-s,y})\,dx\,dy\right]^2 + \left[\iint_S \sin(\phi_{x,y} - \phi_{x-s,y})\,dx\,dy\right]^2} \quad \ldots (3.2)$$

and

$$\Phi = \tan^{-1}\left[\frac{\iint_S \sin(\phi_{x,y} - \phi_{x-s,y})\,dx\,dy}{\iint_S \cos(\phi_{x,y} - \phi_{x-s,y})\,dx\,dy}\right] . \quad (3.3)$$

The contrast in the image is now

$$T(s) = D/C \quad (3.4)$$

and the pattern has a resultant phase shift Φ. Both these factors can be calculated if the phase difference $[\phi_{x,y} - \phi_{x-s,y}]$ is known, and hence the required transfer function curve of contrast and phase shift against the spatial frequency variable s (see Section 4.4) can be plotted.

This simple derivation of the optical transfer function formulae applies strictly to axial imagery. However, the more detailed treatment of Hopkins shows that the same formulae may be applied when the point P of Fig.5 lies well away from the optical axis EG'. In this case, distances in the image plane are referred to the intersection point of the principal ray with the image plane as origin.

4 METHOD OF COMPUTATION

4.1 Calculation of wavefront aberration

The determination of the required phase differences in the exit pupil requires a knowledge of the wavefront aberration[5] of the lens system. Fig.6 shows a distorted wavefront (solid line) passing through the exit pupil of a system, and the reference sphere (dotted line) which has the same radius of curvature at the pole E. G', the centre of the reference sphere, is then the paraxial focus of the system.

The line QP represents a ray, necessarily normal to the wavefront, which intersects the reference sphere at M. The distance MQ is the wavefront aberration $W_{x,y}$ and the phase of the disturbance at M leads on that at Q by an amount

$$\phi_{x,y} = \frac{2\pi}{\lambda} MQ = \frac{2\pi}{\lambda} W_{x,y}$$

where λ is the wavelength of the light.

The first part of the computer programme calculates the coefficients $\omega_{m,n}$ of the polynomial

$$\begin{aligned} W_{x,y} = {} & \omega_{11}\, y + \omega_{20}(x^2 + y^2) + \omega_{22}\, y^2 \\ & + \omega_{31}(x^2 + y^2)\, y + \omega_{33}\, y^3 \\ & + \omega_{40}(x^2 + y^2)^2 + \omega_{42}(\omega^2 + y^2)\, y^2 \\ & + \omega_{51}(x^2 + y^2)^2\, y + \omega_{60}(x^2 + y^2)^3 \quad . \end{aligned} \qquad (4.1)$$

To do this, a number (about 20) of rays are traced through the lens system at selected points x,y of the exit pupil. The point of intersection u,v of each ray with the Gaussian image plane is found and the wavefront aberration deduced from this. Fig.6 illustrates the connection between the wave and ray aberration for the simple case of a ray lying wholly in the tangential plane ($x = 0$, $u = 0$).

Sufficient values of the wavefront aberration are thus obtained to enable an accurate determination of the coefficients to be made, using the method of least squares.

The aberration can then be specified at any point of the exit pupil.

4.2 Determination of effective pupil area

The next stage of the programme is concerned with the determination of the shape of the exit pupil, which may be of any form, for off-axis images, according to the type and extent of the vignetting given by the optical system.

An iterative method is used to find the maximum distance, from the centre of the pupil, at which a ray will just pass inside all the apertures of the system in a given azimuth. 15 azimuths are used, and one ray is traced through the system in each case, its starting point being the edge of the paraxial entrance pupil, and its original direction that appropriate to the field angle being considered. The height above the optical axis at which the ray intersects each surface of the system is calculated and compared with the clear radius available. If the height exceeds this radius at any surface, the starting point

is brought nearer the axis by a small increment ε and the ray retraced. This process is repeated until the ray passes through the system, and its coordinates x and y in the exit pupil are recorded as defining a point on the periphery of the exit pupil (Fig.7). The particular surface which limits the ray height is also noted.

The increment ε is chosen to suit the size of the system being investigated: clearly the boundary of a large pupil need not be defined as exactly, in absolute measure, as that of a small pupil, and computing time is thereby reduced. The final result of this part of the programme is a set of 15 coordinates defining points round one half of the pupil periphery, the pupil being symmetrical about the tangential plane shown by the y-axis in Fig.7. The "centre" of the off-axis pupil is taken as the point O midway between the rays 1 and 15.

When the pupil shape has been determined, the effective area occupied by all the source-pairs at the separation s can be found. This is in fact the area common to two overlapping pupil shapes separated by the distance s. It will be clear in Fig.4(b) that this included area has the same shape as the two (identical) areas of Fig.4(a), and the same result applies to non-circular pupils.

4.3 Calculation of transfer function

When the wavefront aberration and exit pupil coordinates of an optical system have been established by ray-tracing, the components T(s) and Φ of the transfer function can be derived as outlined in Section 3 above.

The integrals involved can be evaluated analytically only in the very simplest cases; generally a numerical technique, such as that described below, has to be used.

One simple and very important case which can be solved analytically is that of the in-focus, aberration-free system. Here the phases $\phi_{x,y}$ (equations (3.2) and (3.3)) are all zero and the transfer function reduces to:-

$$T(s) = D/C = \iint_S dx\,dy \Big/ \iint_A dx\,dy \quad ; \quad \Phi = 0 \ .$$

Thus the contrast in the image depends solely on the ratio of the effective to full area of the exit pupil.

This ratio, for a circular pupil, is given by

$$T(s) = \frac{1}{\pi}\left[2\cos^{-1}(s/2) - \sin\{2\cos^{-1}(s/2)\}\right] \ . \qquad (4.2)$$

Values of T(s) versus s for this case are plotted in Fig.8 (solid line).

For the general case of a vignetted pupil, and a full aberration function (see equation (4.1)) the integration is carried out numerically by covering the effective area of the exit pupil with a square mesh (Fig.7), and determining a weighted mean value for the aberration within each square. The number of squares contained within the pupil and within the region of overlap (Fig.4(b)) is calculated, and also the phase difference $(\phi_{x,y} - \phi_{x-s,y})$, of equations (3.2) and (3.3), at a series of points separated by a distance equal to the length of side of the squares, and lying in the overlap region.

Equations (3.2) and (3.3) can then be applied to find the transfer function, the integrals now becoming sums, the number of terms in which are equal to the number of squares within the overlap region. The constant term C (equation (3.1)) is of course represented by the number of squares in the complete pupil.

The accuracy of the final result is clearly dependent on the size of the mesh. Fig.8 illustrates the kind of errors which arise from the finite size of square, when the transfer function of an aberration-free lens is calculated by this numerical process. The original computer programme has since been modified so that the number of squares contained in the effective area is never less than 1000, the square size decreasing as the separation s increases. Under these circumstances the error in T(s) should never exceed 0.01.

This description of the theory underlying the computer programme has assumed a horizontal separation of secondary sources, that is to say an orientation of the object grating so that its lines lie radially in the lens field (parallel to the y-axis in Fig.7).

However, the same techniques may be used to calculate the response for any other orientation of the grating, and in practice the programme caters for orientations of 0° (radial lines), 90° (tangential lines), and any angle between these.

4.4 Relation of spatial frequency to the variable s

It has already been shown that the spatial frequency of the lines in the image plane depends on the separation s of the secondary sources in the exit pupil.

The frequency is usually expressed as the number of lines per millimeter in the image plane.

Equation (3.1) above shows that the intensity repeats its value at distances $u = 2\pi/s$ apart in this plane, and this is therefore the "spatial wavelength" of

the sinusoidal pattern. Coordinates in the exit pupil are actually expressed as fractions of its maximum radius (specifically the radius of the paraxial pupil - see Appendix) and s is of course in the same units. If S is the actual separation of the sources, the fractional value is:

$$s = \frac{S}{X_{max}} \qquad (4.3)$$

where X_{max} represents the maximum pupil radius (see Fig.5). Distances in the image plane are also expressed in "reduced" coordinates viz:-

$$u = \frac{2\pi g}{R\lambda} X_{max} \qquad \text{(Appendix - Equation (A.1))}$$

so that the intensity repeats at intervals

$$u = \frac{2\pi}{s} = \frac{2\pi}{R\lambda} g \; X_{max}$$

g is the <u>actual</u> length of one period in the image plane, and the spatial frequency ν is given by

$$\nu = 1/g = \frac{X_{max}}{R\lambda} s \; .$$

In the commonest case, that of a photographic lens with the object at infinity:

$$\nu = \frac{1}{2\lambda(F/no.)} s \; . \qquad (4.4)$$

The maximum source separation which will provide a fringe pattern in the image plane, is equal to the diameter of the exit pupil. Thus in the expression (4.3) above, $S_{max} = 2 X_{max}$ and $s_{max} = 2$.

This represents the ultimate resolution limit of the optical system, since with wider separations only one source lies within the aperture at a time, and the illumination of the focal plane is uniform. For a relative aperture of f/8, and a wavelength of 5×10^{-4} mm, this limit is reached at $\nu = 250$ ℓ/mm.

5 TRANSFER FUNCTIONS IN "WHITE LIGHT"

The foregoing discussion refers, of course, to monochromatic illumination of the object. In most practical cases a continuous spectrum is involved, and the problem remains of synthesising the transfer function applying in these

conditions from the results calculated at a number of discrete wavelengths. In principle, this can be done by adding corresponding ordinates of these "monochromatic" response curves, after multiplying each by a factor proportional to the intensity or sensitivity of the light source and receiver (photographic film, television tube etc) taking account of the relative spatial phase at each wavelength.

In practice, two main problems arise: firstly, how many separate wavelengths need be specified to yield an accurate "white light" result, and secondly what is the most efficient method of selecting the best image plane in which to find the "combined" transfer function.

These points are under investigation at the time of writing, and the results reported in the second half of this Report refer only to monochromatic light.

6 OPERATION OF COMPUTER PROGRAMMES

6.1 Introduction

The three sub-programmes to be described (designated A, B and F) cover three separate phases of the calculation of optical transfer functions.

Programme A takes the lens design data and calculates the wavefront aberration and the shape of the exit pupil, for given object/image conjugates and field angles.

Selection of the best focal plane in which to calculate the transfer function is done by means of programme B, and programme F determines the contrast and phase curves in the chosen focal plane, at the given field angle.

The programmes are written in Mercury Autocode; programme F has recently been modified slightly to enable it to be used on the "Atlas" computer. "Atlas" is about 60 times faster than "Mercury" and has a greater storage capacity; this allows the use of a smaller mesh size, and hence an increase in accuracy (see Section 4.3).

The operation of these programmes will be illustrated by means of an example, viz. a 24 inch f/5.6 reconnaissance lens of new design. It will be shown how the designer's data are used in programme A, and the way in which the results from this are used in programmes B and F.

6.2 Programme A: Calculation of wavefront aberration and pupil shape

This programme calculates the wavefront aberration (Section 4.1) for three wavelengths both for the axial case and for one selected field angle. The pupil

shape for this angle is given in the form of 15 coordinates (x,y) round half the pupil, which is symmetrical about the y-axis (Fig.7). As mentioned previously the x,y actually used are "reduced" coordinates obtained by dividing actual distances from the axes by the radius of the exit pupil*.

Fig.9 shows the data as received from the lens designer, and Fig.10 the form of the data tape produced from this. In counting the number of surfaces, the stop is included, and where two surfaces are cemented together only one is counted.

Starting values for a paraxial marginal ray have to be chosen, u being the angle the ray makes with the optical axis, and h the height above the axis of the edge of the paraxial entrance pupil. The sign convention used for the angle is that an anti-clockwise rotation from ray to axis denotes a positive angle. With object at infinity, u = 0 and h = (focal length)/2(f/no.). With a finite object distance u and h must be deduced from simple paraxial considerations.

As explained in Section 4.2, the accuracy ε to which the shape of the exit pupil needs to be defined depends on the actual size of the system. The condition that a ray shall pass through a given surface is

$$\rho < (\text{Free aperture}) + \varepsilon$$

where ρ is the distance between the optical axis and the point at which the ray intersects the surface.

Refractive indices for commonly used wavelengths can be obtained directly from the glass catalogue; other wavelengths can be interpolated using a suitable dispersion formula[7].

The field angle θ can have any value other than 0° and the Lagrange invariant (H) is given by:-

$$H = h \tan \theta$$

when the field angle is measured from the centre of the paraxial entrance pupil for a finite object distance.

The programme tape takes about 6 minutes to be read into Mercury. Each set of data takes about 2 minutes to calculate.

---

*Strictly, the radius of the pupil, in the sagittal plane, calculated by paraxial formulae.

At the end of a set of data, the machine will return to the beginning of the programme, so that for results for another field angle, the complete set of design data must be read in again.

Fig.11 shows the form in which the results are presented.

The "reduced height of exit pupil" gives the ratio of the actual on-axis pupil radius, to that of the paraxial pupil. Under "pupil shape", Q defines which of the 15 "peripheral rays" is being considered (see Fig.7), S denotes the surfaces which limit the off-axis beam in this azimuth (more than one surface may limit a ray within the tolerance ε) and X' and Y' give the coordinates of the exit pupil periphery.

The "exit pupil scale ratio" gives the relationship between the numerical apertures of the off-axis and on-axis exit pupils. This ratio is used in the later programmes.

The coefficients of wavefront aberration ω_{11} to ω_{60} are given in numbers of wavelengths at each of the three chosen wavelengths. The reference sphere is centred on the paraxial focus for the mean wavelength (wavelength 0) in the axial case, or on the point at which the principal ray intersects the image plane containing the paraxial focus, for the extra-axial case.

If, during the ray-tracing procedures involved in the execution of the programme, one of a number of unacceptable conditions occurs, the computation stops. The nature of the fault is printed out, and the programme is returned to the starting point ready to read a fresh set of data. The unacceptable conditions are:-

(a) "Total reflection occurs".

(b) "Surface radius insufficient to allow ray through": on a highly curved surface, the ray fails to intersect the sphere of which the surface forms part.

(c) "Marginal ray fails to pass": initial value of h set too large.

(d) Certain numerical errors in computation.

In each case, the surface and the ray involved are also quoted.

6.3 Programme B: Selection of "best focus"

This programme calculates the transfer function on the axis of a system for different focal planes, at a particular spatial frequency. This allows the region of "best focus" to be located, for use in the subsequent calculations. It should

be noted that this programme can be used independently of programme A, so that if, for example, the wavefront aberration of a manufactured lens has been measured, the axial transfer factor for the given frequency can be calculated.

Fig.12 shows the layout of the input data.

The system number can have any value and is only used to differentiate between cases.

The numerical aperture in the image space is equal to $\sin \alpha'$ (Fig.6) or (1/2(F/no.) for an object at infinity.

A value for s is chosen by considering which frequency is of predominant importance in the particular application of the lens system. For example, a spatial frequency of between 20 ℓ/mm and 40 ℓ/mm would be an appropriate choice for an aerial reconnaissance lens, which would normally yield photographic resolutions within this range on the most commonly used emulsions. An equivalent form for equation (4.4) above is

$$s = \frac{\lambda}{\sin \alpha'} \nu \qquad (6.1)$$

and this can be used to calculate the spatial frequency variable (corresponding to ν lines per millimeter) for any object/image conjugates. In the very rare case in which the image plane is immersed in a medium other than air, the appropriate refractive index (n) appears in the denominator of equation (6.1).

The interval between focal planes, specified by the "defocus aberration" term $\Delta\omega_{20}$, is related to the actual distance ΔZ by the formula

$$\Delta\omega_{20} = \frac{n \sin^2 \alpha'}{2\lambda} \Delta Z \qquad (6.2)$$

for shifts of focus which are small compared to the focal length. The upper and lower limits of the range of focus positions are set by choosing an appropriate number of these intervals each side of the paraxial focus.

In accordance with the sign convention used throughout this Report, distances ΔZ measured away from the lens system in the image space are counted as positive.

The programme tape is read into Mercury in about 2 min. Execution time is about 1 min for 10 values of ω_{20}.

The asterisk at the end of each set of data causes the machine to return to the beginning of the programme ready to read a complete new set of data. If

there is no asterisk the machine will expect to read another set of the last 6 values only (from s onwards).

Fig.13 shows the way in which the results are printed out. "S/A" gives the ratio of "effective" to actual area of the (circular) pupil. In this example the response T(s,0) is seen to be highest at $\omega_{20} \simeq -1.86$ or 0.27 mm from the paraxial focus ($\omega_{20} = 0$) for this wavelength, and nearer the lens.

6.4 Programme F. Determination of transfer function curves

After selection of the region of optimum focus on axis, transfer functions, in image planes intersecting the axis in this region, can be calculated. Programme F carries out this calculation, deriving the amplitude and phase curves for a selected range of spatial frequencies; the field angle, image plane and line orientation (see end of Section 4.3) being specified.

As previously mentioned, for good accuracy this programme should be run on "Atlas", or a machine (accepting the Mercury Autocode) which has quick access storage capacity of at least 7000 long numbers.

Fig.14 shows the layout of the data tape. In calculating the axial transfer function the coordinates for a circular pupil are used (see inset to Fig.14) after multiplication by the reduced height of exit pupil given in the output of programme A.

The aberration coefficients are taken directly from programme A results with the exception of ω_{20} which must be given the value indicated by programme B. If $\delta\omega_{20}$ is the difference between paraxial and "optimum" focus on axis, the corresponding value off-axis, for field-angle θ is given by

$$\delta\bar{\omega}_{20} = \sec\theta \text{ (exit pupil scale ratio) } \delta\omega_{20} \ .$$

That is to say, $\delta\bar{\omega}_{20}$ represents the shift of focus, along the principal ray, which is required to move from the paraxial image plane (to which the coefficients in programme A results are referred) to the "optimum" image plane. This value is inserted in the data for programme F. Results for other image planes in the neighbourhood of the "optimum" one can of course be obtained by changing this value of $\delta\bar{\omega}_{20}$ appropriately. In calculating the axial response all the coefficients except ω_{20}, ω_{40} and ω_{60} are put equal to zero. Azimuth angles normally specified are 0°, for radial lines, 90° (tangential lines) and 45°.

Atlas takes about 6 sec to read the programme and about 30 sec to produce both amplitude and phase results for 10 values of s. At the time of writing the

programme will only cater for one complete set of data at a time - the asterisk returning the machine to the beginning of the programme ready to read in a complete new set of data. It is planned, however, to alter the programme to make it possible to feed in more than one azimuth angle, at a given field angle and focus position, without repeating the rest of the data.

Fig.15 shows the form of the output from the machine. The column headed "E" gives the length of side of squares in the mesh used in the integration, (Section 4.3) on the "reduced" scale which gives a maximum pupil radius of unity. s/A is again the ratio of effective to actual pupil areas, and $T(s,\phi)$ the modulus of the optical transfer function, derived from the real and imaginery parts (or cosine and sine functions in equations (3.2) and (3.3)) shown.

7 RESULTS

Some results of the calculation of the 24 inch lens are shown in Fig.16. These refer to monochromatic light of the helium "d" line - 5876 Å. The solid curve in Fig.16(a) shows the modulation transfer function at the focal point on the optical axis giving maximum response at 40 ℓ/mm. The phase (360° corresponding to one line spacing) is zero throughout, as indicated by the horizontal line. For comparison, the modulation curve for an aberration-free lens is also shown (dotted line) together with the results of measurements on an actual lens. The marked disparity between the latter and the calculated curve illustrates the extent to which small manufacturing errors may detract from the theoretically available performance. Although work of the highest precision obtainable by traditional methods is involved here, it is clear that much more can be extracted from a modern, highly corrected, design such as this. Techniques for improving optical manufacture are under current investigation, and in this work new and more sensitive methods of assessment such as the optical transfer function are proving their value.

Fig.16(b) shows calculated curves for the same focal plane as in 16(a), but for an image point 12° from the optical axis. The contrast for radial lines of all spatial frequencies has been reduced (from that on axis) and even more so for tangential lines. The phase part (dotted) of the transfer function for tangential lines shows simply an abrupt change from 0 to 180° or vice-versa, when the contrast falls to zero. This is characteristic of "spurious resolution" which would be observed for spatial frequencies between 15 and 35 ℓ/mm and between 60 and 80 ℓ/mm. The absence of any curvature in the phase function (except for a very slight effect above 60 ℓ/mm) indicates a good correction for unsymmetrical "coma" type aberrations.

8 ACKNOWLEDGEMENTS

The work of writing and testing the programme was carried out by Mr. B.J. Hindley under a Ministry of Aviation Research Agreement with Imperial College. The basic theory and the principles of the numerical calculation were introduced and developed by Dr. H.H. Hopkins, who also supervised the testing of the programme. I. & E.E. Dept cooperated in the running of trials on the R.A.E. "Mercury" computer.

Appendix

DERIVATION OF THE BASIC DIFFRACTION FORMULAE

The contribution, of an element of the wavefront passing through the exit pupil of an optical system, to the amplitude in the image plane may be calculated using Huygen's principle. The element is then regarded as a source of spherical, simple-harmonic waves, and the simple formulae describing the propagation of such a wave may be applied[6].

Thus, if K represents the amplitude of the wavefront over the element $\delta X\ \delta Y$ (Fig.5), we may write for the amplitude at P, at time t

$$\delta A = \frac{K}{r} \cos\left[\frac{2\pi}{\lambda}(ct - r)\right]$$

where r is the distance between the element and the point P, and λ the wavelength of the light.

Suppose initially that the parent wavefront is spherical and centred at G'. Then, provided P is very close to G', the distance r is practically constant whichever element of the wavefront is chosen. The denominator of the above expression can therefore be regarded as constant, but not the factor r within the cosine, since small variations here can have large effects on the value of the complete expression.

Since we are concerned with conditions at a particular instant of time, t is constant, and putting the expression, for convenience, into complex notation we have:-

$$\delta A = [\text{constant}] \times K\, e^{-\frac{i2\pi}{\lambda} r} .$$

Now, it is easily shown that

$$r = R - Xg/R - Yh/R$$

where R is the radius of curvature of the (spherical) wavefront and g,h the coordinates of the point P (Fig.5). Putting the former with the other constants we therefore have

$$\delta A = [\text{constant}] \times K\, e^{i\frac{2\pi}{\lambda}(Xg/R+Yh/R)} .$$

It is convenient to change the scale of the pupil and image-plane coordinates so that they become dimensionless, viz:-

$$x = X/X_{max} \quad \text{and} \quad u = 2\pi g\, X_{max}/R\lambda \qquad (A.1)$$

$$y = Y/Y_{max} \qquad v = 2\pi h\, Y_{max}/R\lambda \ .$$

(i.e. $x = y = 1$ at edge of pupil.)

Since we are also mainly interested in relative amplitude, the scale on which this is measured can also be altered to eliminate the constant. With these substitutions the amplitude contribution becomes:-

$$\delta A = K\, e^{i(ux+vy)} \ .$$

If the wavefront has aberration, and is not spherical (see Fig.6) the above expression can still be used provided the phase difference $\phi_{x,y}$, between the wavefront and a reference sphere of radius R, is known. At the instant of time considered, the disturbance in the reference surface is greater or less than that in the actual wavefront, depending on this phase difference, and one may write for the amplitude in the reference sphere:-

$$K = \text{constant} \times e^{i\phi_{x,y}}$$

or

$$\delta A = e^{i\phi_{x,y}}\, e^{i(ux+vy)} \qquad (A.2)$$

again scaling the amplitude to eliminate constants.

REFERENCES

No.	Author	Title, etc
1	J.M. Naish A.C. Marchant	Measurement of the response function of an optical system. R.A.E. Tech. Note No. Ph 493, January 1956
2	F.H. Perrin	Methods of appraising photographic systems. Jour. Motion Picture and Television Engineers, Vol.69, pp.151-6 and 239-248, 1960
3	L.C. Martin	Technical Optics, Vol.II, p.104, Pitman, 1950
4	H.H. Hopkins	The frequency response of optical systems. Proc. Physical Soc., Vol.69(B), p.562, 1956
5	H.H. Hopkins	Wave Theory of Aberrations, O.U.P., 1950
6	R.S. Longhurst	Geometrical and Physical Optics, p.2, Longmans, 1957
7	Herzberger	Modern Geometrical Optics, p.120, Interscience Inc., 1958

Fig.1

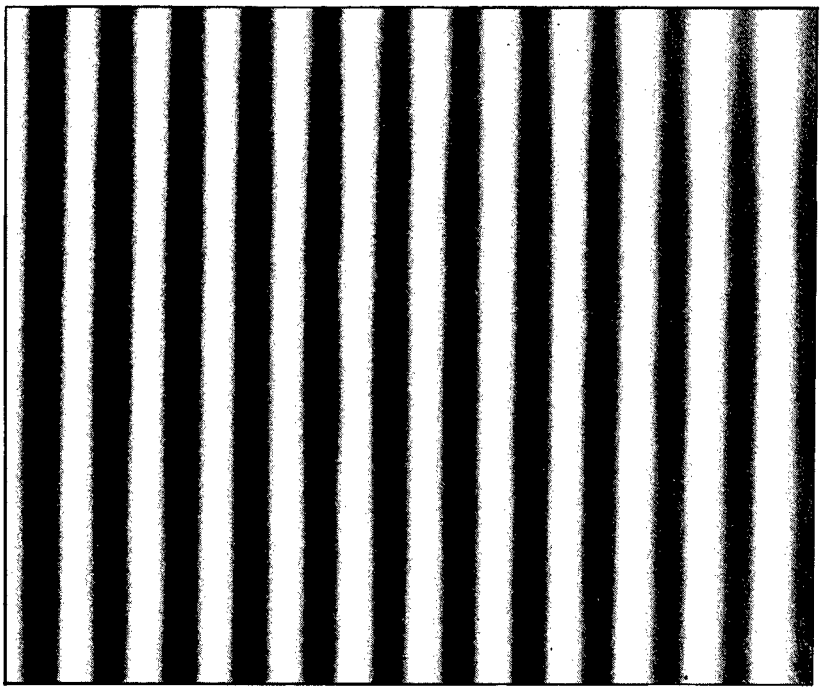

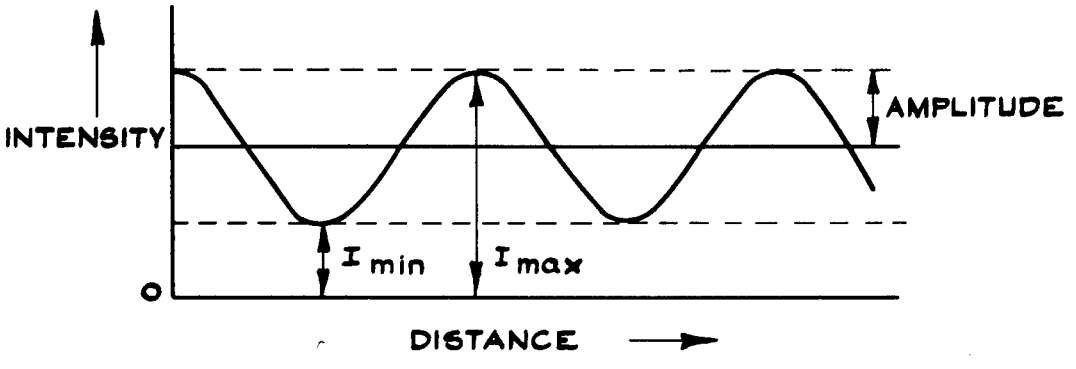

FIG. 1 OPTICAL "SIGNAL"

Fig.2

IEE 6628

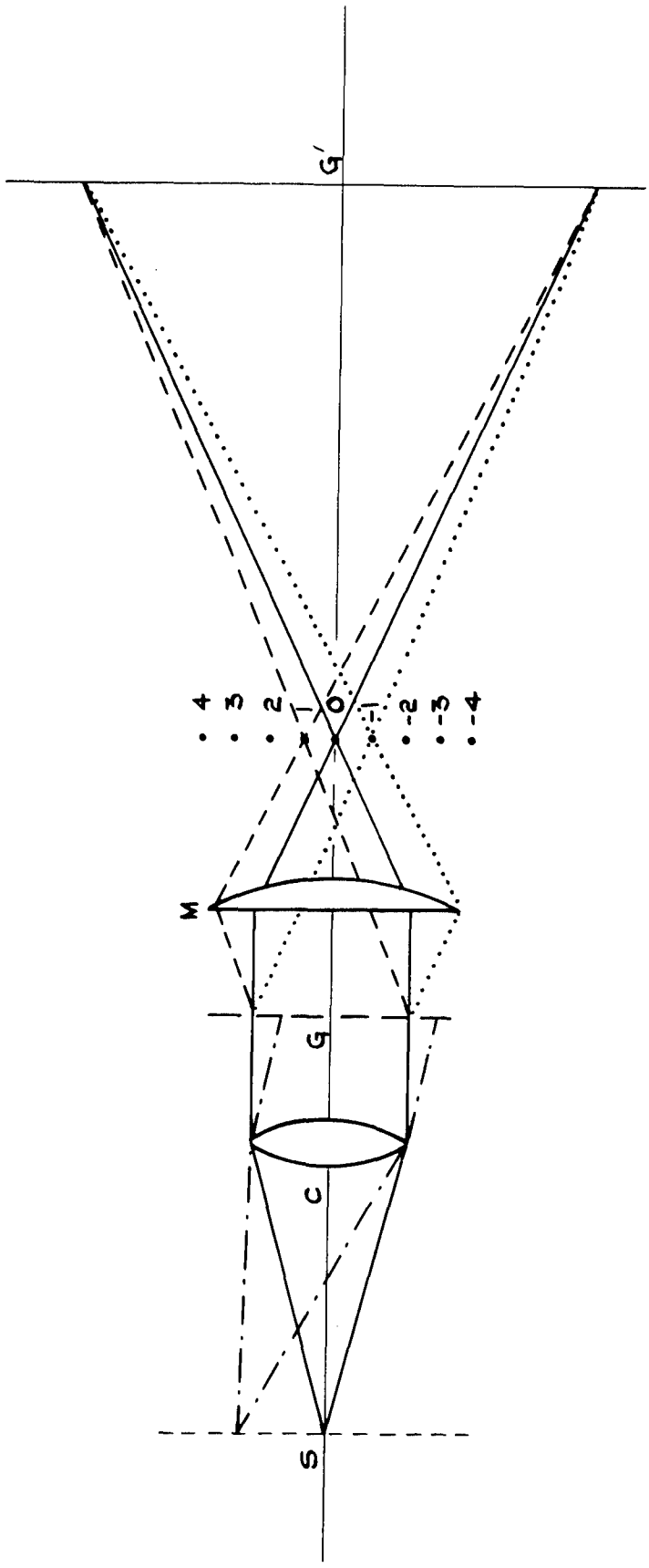

FIG. 2 ABBE THEORY OF IMAGERY

Fig.3

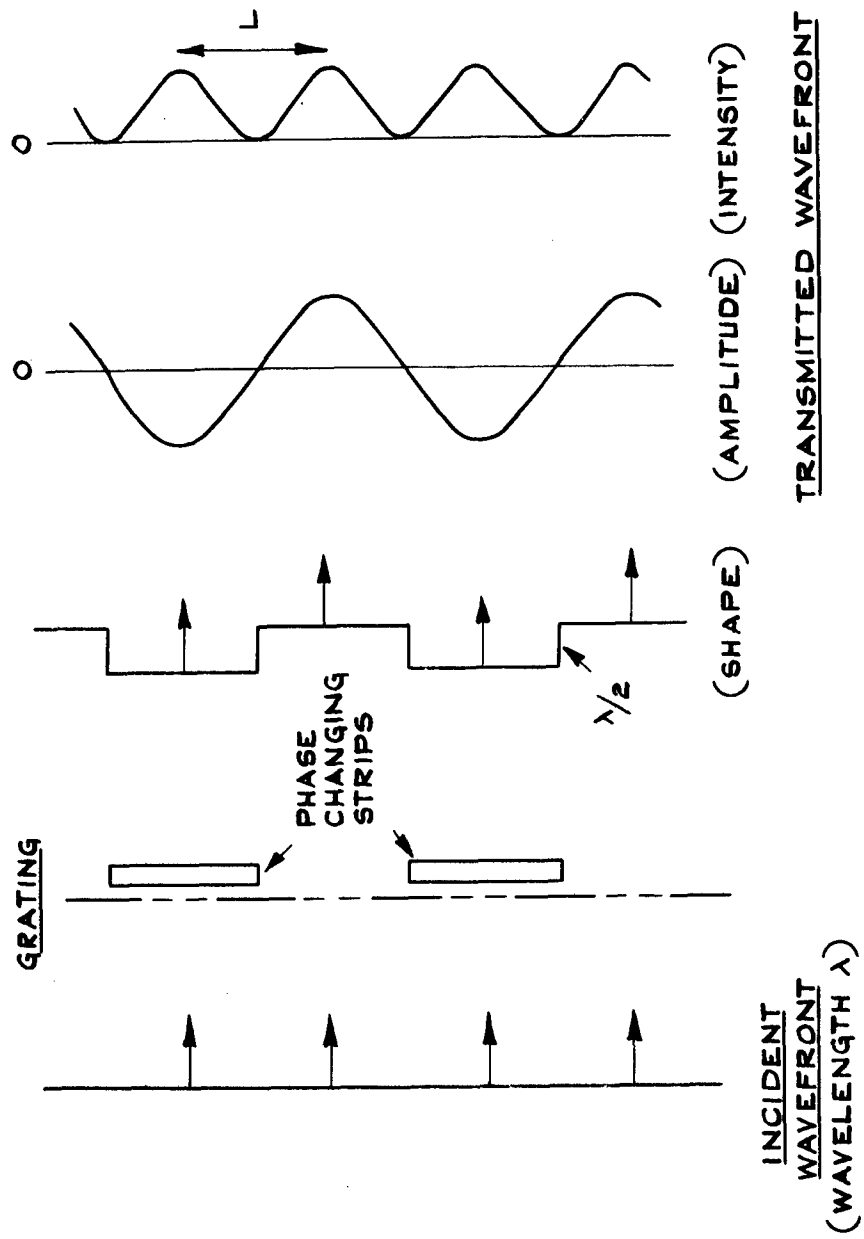

FIG. 3 "SINUSOIDAL" GRATING

Fig.4

IEE 6630

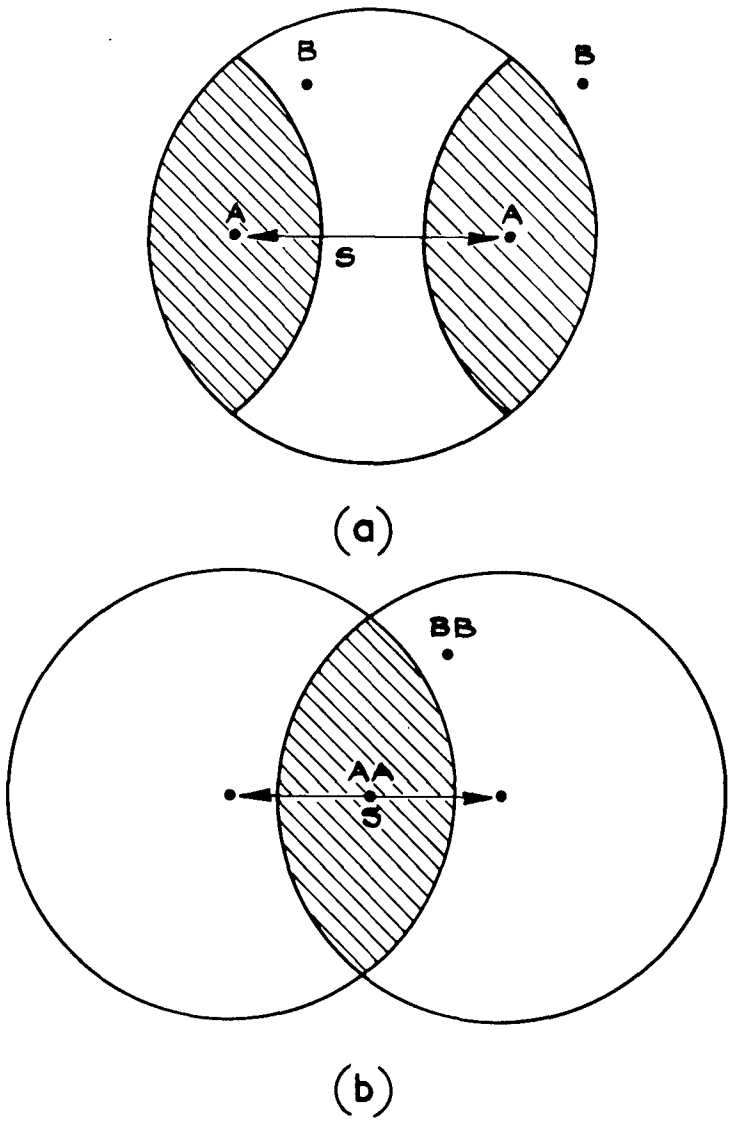

FIG. 4 (a & b) EFFECTIVE PUPIL AREAS

Fig.5

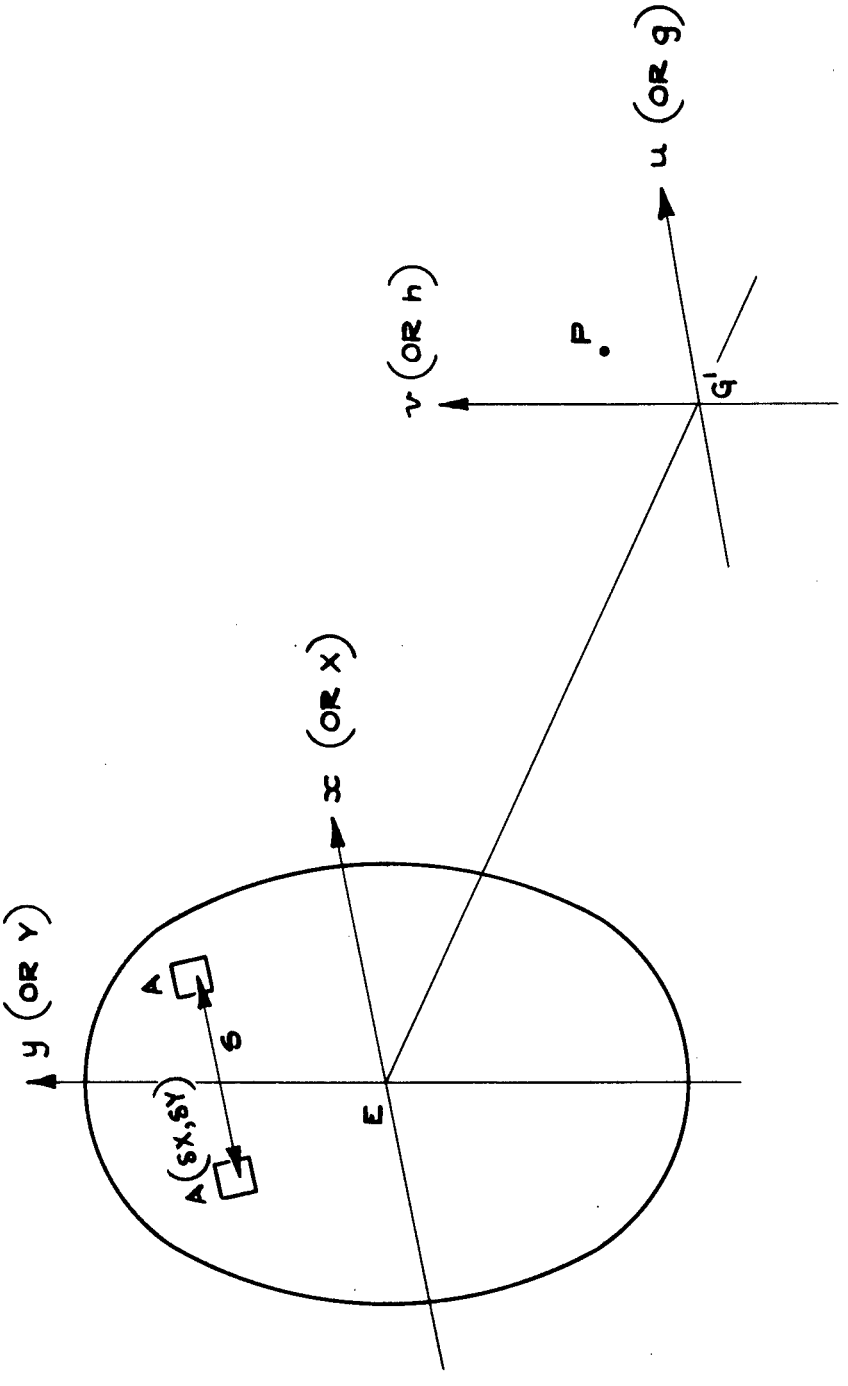

FIG. 5 SCHEME FOR DERIVATION OF BASIC FORMULAE

Fig.6

IEE 6632

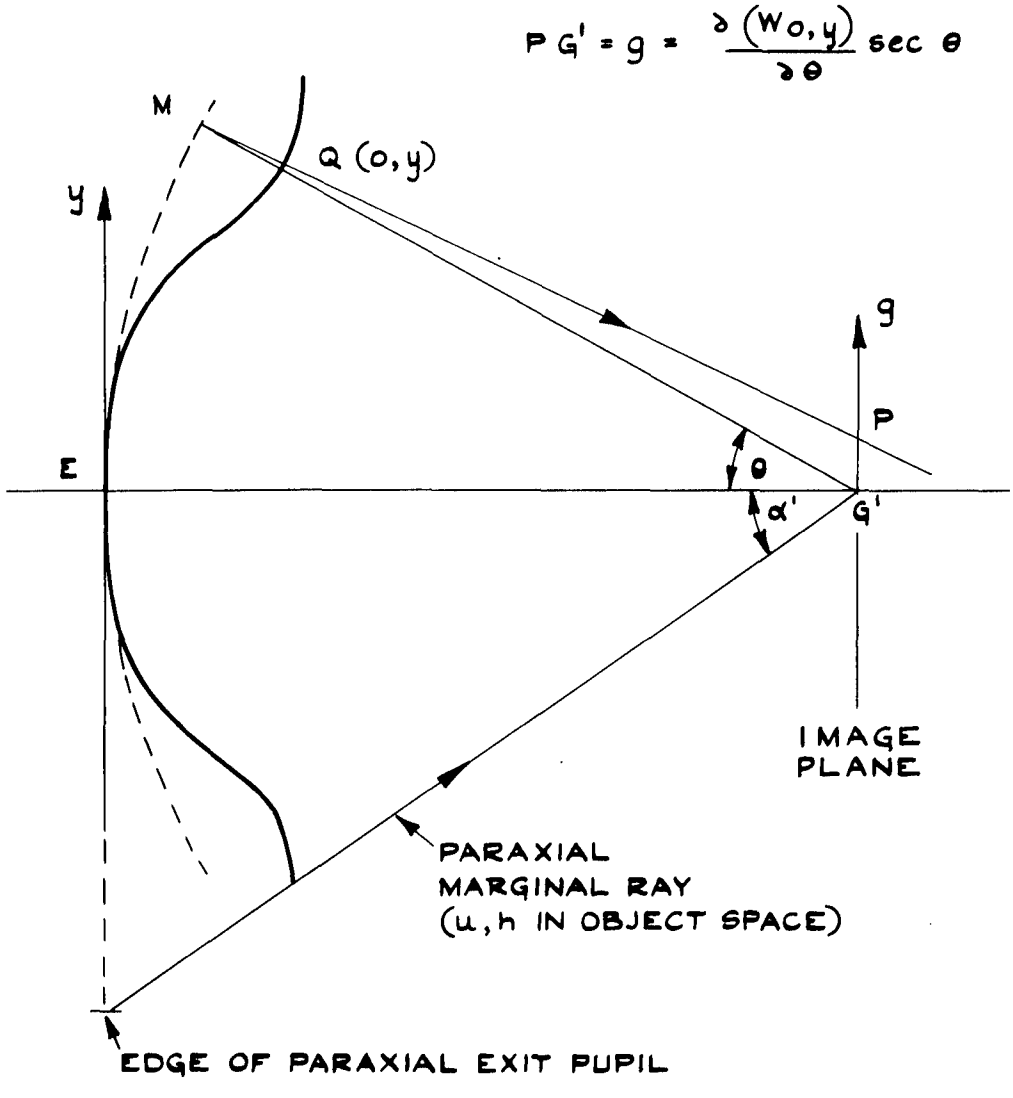

FIG. 6 CONNECTION BETWEEN WAVEFRONT ABERRATION AND RAY DISPLACEMENT

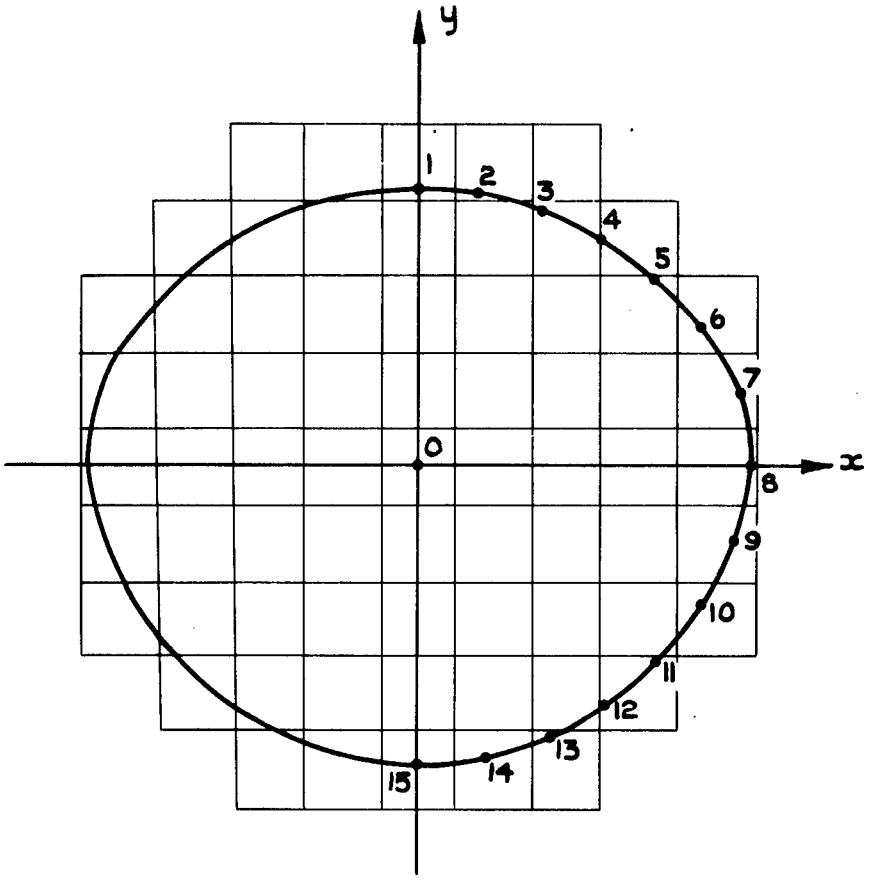

FIG. 7 METHOD OF DEFINING EXIT PUPIL

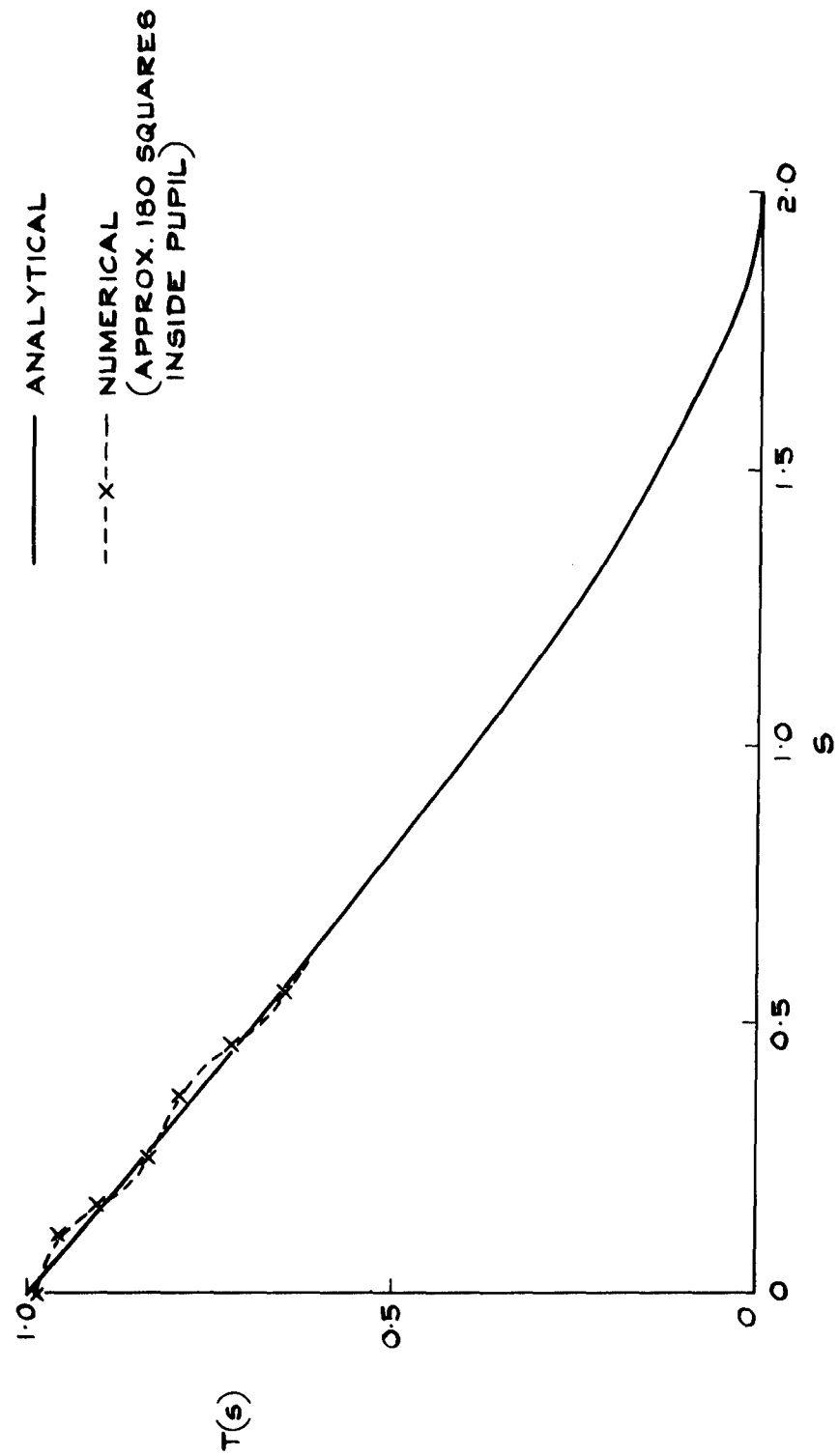

FIG. 8 OPTICAL TRANSFER FUNCTION OF ABERRATION-FREE LENS

Fig.9

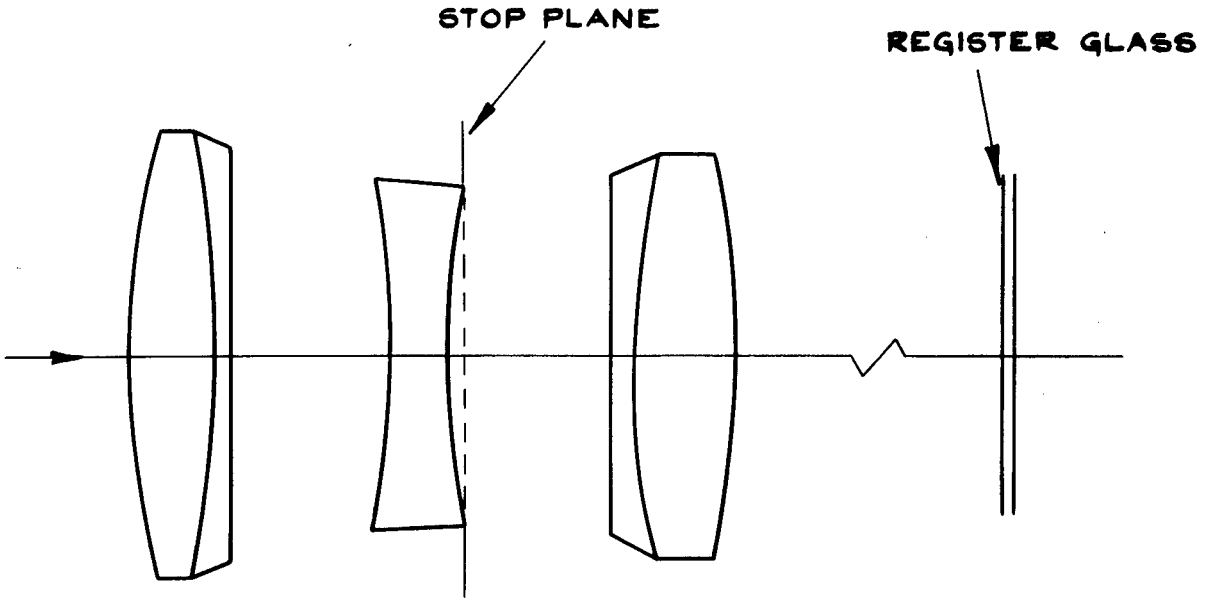

SURFACE	CURVATURE ($mm^{-1} \times 10^3$)	SEPARATIONS (mm)	CLEAR DIAM. (mm)	n_d	$n_e - n_d$ ($\times 10^3$)	$n_{A'} - n_d$ ($\times 10^3$)
				1	0	0
1	4·5370	22·747	119·2	1·71991	3·43	-9·22
2	-3·5658	6·499	119·2	1·61329	3·31	-8·88
3	0·8484	41·256	106·0	1	0	0
4	-3·6217	17·287	89·4	1·62130	4·05	-10·45
5	4·8314	8·000	87·2	1	0	0
6 (STOP)	0	35·934	88·0 *	1	0	0
7	-0·4702	6·174	93·8	1·61342	3·31	-8·86
8	4·6538	26·191	106·4	1·72078	3·41	-9·17
9	-4·1482	509·160	106·4	1	0	0
10 } (REG.	0	6·35	(457·2	1·5230	2·12	-5·81
11 } GLASS)	0		457·2)	1	0	0

* STOP SETTING FOR F/5·6

FIG. 9 EXAMPLE OF LENS DESIGN DATA
(24" F/5·6 — B.P. 954585 : C.G. WYNNE/ N.R.D.C.)

FIG.10 FORM OF DATA TAPE FOR PROGRAMME A
(Explanations in brackets)

Blank Tape
24 in. F/5.6 (Man. Data) [Title: must be terminated with Carriage Return, Line Feed]

Blank Tape

11 [No. of surfaces]

6 [Stop surface number]

0 [u in radians] } Starting data for paraxial marginal ray
53.058929 [h] }

0.5 [Tolerance ε to be used in determination of pupil radius - see Section 6.2]

0.0005876 [Mean wavelength (λ_0) in mm]

1
1.71991
1.61329
1
1.62130
1
1
1.61342
1.72078
1
1.52400
1

} [Refractive indices (n_0) for λ_0 - including external media]

0.0005461 [Wavelength (λ_1) in mm]

0
0.00343
0.00331
0
0.00405
0
0
0.00331
0.00341
0
0.00212
0

} [Partial dispersions ($n_1 - n_0$)]

0.0007682 [Wavelength (λ_2) in mm]

0
-0.00922
-0.00888

0

0.0007682 [Wavelength (λ_2) in mm]

0
-0.00922
-0.00888
0
-0.01048
0
0
-0.00888
-0.00917
0
-0.00581
0

[Partial dispersions ($n_2 - n_0$)]

22.747
6.499
41.256
17.287
8.00
35.934
6.174
26.191
509.16
6.35

[Separations in mm]

0.0045370
-0.0035658
0.0008484
-0.0036217
0.0048314
0
-0.0004702
0.0046538
-0.0041482
0
0

[Curvatures in mm^{-1}: Positive if centre of curvature is to right of surface, with light incident from left - see Fig.9]

59.6
59.6
53.0
44.7
43.6
44.0
46.9
53.2
53.2
228.6
228.6

[Free apertures in mm]

12 [Field angle in degrees]

11.278026 [Lagrange Invariant]

FIG.11 RESULTS FROM PROGRAMME A

24 in. F/5.6 (Man. Data)

Wavelength (0) = 5.8760, -4
Wavelength (1) = 5.4610, -4
Wavelength (2) = 7.6820, -4

Reduced height of exit pupil = 1.00

Axis abn. coeffts.

	(1)		(0)		(2)	
W(2,0)	1.5821,	0	0.0000,	0	-7.4008,	0
W(4,0)	5.1641,	0	5.5842,	0	5.7077,	0
W(6,0)	-4.7360,	0	-4.2997,	0	-3.0943,	0

Exit pupil scale ratio = 0.9841

Field angle = 12.00 degrees.

Pupil shape

Q	S	X'	Y'
1	7	0.00	0.76
2	7	0.18	0.73
3	7	0.35	0.69
4	7	0.52	0.62
5	7	0.67	0.51
6	7	0.81	0.37
7	7	0.92	0.20
8	3		
	4		
	6		
	7	1.00	-0.00
9	3	0.93	-0.20
10	3	0.81	-0.38
11	3	0.67	-0.51
12	3	0.52	-0.62
13	1		
	3	0.35	-0.69
14	1		
	3	0.18	-0.74
15	1		
	3	0.00	-0.75

Aberrn. coeffts.

	(1)		(0)		(2)	
W(1,1)	9.3080,	-3	1.5099,	-1	6.0239,	-1
W(2,0)	4.9354,	0	3.4798,	0	-4.0567,	0
W(2,2)	-4.1933,	0	-3.9636,	0	-3.4744,	0
W(3,1)	2.2565,	0	1.9996,	0	1.4068,	0
W(3,3)	-1.0080,	0	-9.1831,	-1	-6.5926,	-1
W(4,0)	3.3447,	0	3.9271,	0	4.5065,	0
W(4,2)	2.0455,	0	2.0085,	0	1.7253,	0
W(5,1)	-1.1850,	0	-1.1407,	0	-9.4684,	-1
W(6,0)	-5.1869,	0	-4.7174,	0	-3.4134,	0

FIG.12 DATA FOR PROGRAMME B
(Explanations in brackets)

Blank tape

1	[System no.]
15	[No. of points defining pupil periphery (Fig.7)]
0.089285	[Numerical aperture in image space]
5876	[Wavelength in Angströms]
0.263	[Spatial Frequency s]
5.5842	[$W_{4,0}$ from Prog. A results: Axis Abn. Coeffts.]
-4.2997	[$W_{6,0}$ from Prog. A results: Axis Abn. Coeffts.]
-3.44	[$W_{2,0}$ corresponding to focal plane nearest lens]
3.44	[$W_{2,0}$ corresponding to focal plane farthest from lens]
0.344	[Interval $\Delta W_{2,0}$ between focal planes]
*	[Asterisk]

FIG.13 RESULTS FROM PROGRAMME B

Freq. response B.

Freq. response curves

System 1

Axial calculation

Tests for best focal plane

Wavelength = 5876

Azimuth (0)

s = 0.26*

S/A = 0.84

W(6,0) = -4.30 , W(4,0) = 5.58

W(2,0)	T(s,0)
-3.44	-0.00
-3.10	0.15
-2.75	0.33
-2.41	0.49
-2.06	0.60
-1.72	0.61
-1.38	0.52
-1.03	0.36
-0.69	0.19
-0.34	0.06
-0.00	0.01
0.34	0.04
0.69	0.10
1.03	0.14
1.38	0.13
1.72	0.06
2.06	-0.01
2.41	-0.06
2.75	-0.05
3.10	-0.01
3.44	0.04

* (40 ℓ/mm)

FIG.14 DATA FOR PROGRAMME F
(Explanations in brackets)

Blank tape

24 in. F/5.6, Field angle = 12, Best Focus[/]

Blank tape

15 [No. of points defining pupil periphery]

0	0.76
0.18	0.73
0.35	0.69
0.52	0.62
0.67	0.51
0.81	0.37
0.92	0.20
1	0
0.93	-0.20
0.81	-0.38
0.67	-0.51
0.52	-0.62
0.35	-0.69
0.18	-0.74
0	-0.75

} [Coordinates of pupil periphery] ——

[Coordinates of circular (axial) pupil:-

0	1
0.22	0.97
0.43	0.90
0.62	0.78
0.78	0.62
0.90	0.43
0.97	0.22
1	0
0.97	-0.22
0.90	-0.43
0.78	-0.62
0.62	-0.78
0.43	-0.90
0.22	-0.97
0	-1

]

5876 - [Wavelength - Angström units]

0.15099	
-1.87000	
-3.96360	
1.99960	
-0.91831	[Aberration coeffts.]
3.92710	
2.00850	
-1.14070	
-4.71740	

0	[Initial value of s]
0.526	[Final value of s]
0.0526	[Interval between successive values of s]
90	[Azimuth angle in degrees]
*	[Asterisk]

[/] Title must be terminated by Carriage Return, Line Feed.

FIG.15 RESULTS FROM PROGRAMME F

24 in. F/5.6, Field angle = 12, Best Focus

Wavelength = 5876

Azimuth = 90.00

E	s	S/A	Real	Imag.	T(s,ϕ)	Phase
0.045	0.000	1.000	1.002	0.000	1.002	0.000
0.045	0.053	0.953	0.562	0.111	0.573	0.195
0.040	0.105	0.909	-0.031	-0.010	0.033	-2.821
0.040	0.158	0.859	-0.197	-0.139	0.241	-2.529
0.040	0.210	0.815	-0.069	-0.076	0.103	-2.308
0.040	0.263	0.772	0.039	0.059	0.070	0.988
0.035	0.316	0.721	0.041	0.091	0.100	1.148
0.035	0.368	0.678	0.008	0.035	0.036	1.350
0.035	0.421	0.636	-0.002	-0.022	0.022	-1.667
0.035	0.473	0.591	-0.001	-0.036	0.036	-1.599
0.030	0.526	0.551	0.003	-0.022	0.022	-1.434

Fig.16

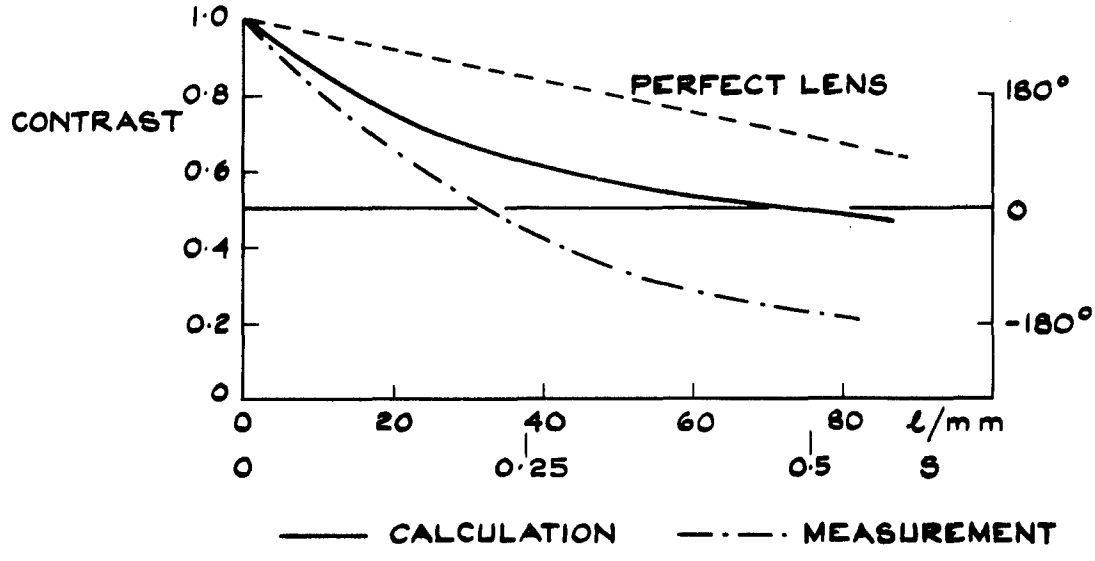

(a) ON AXIS

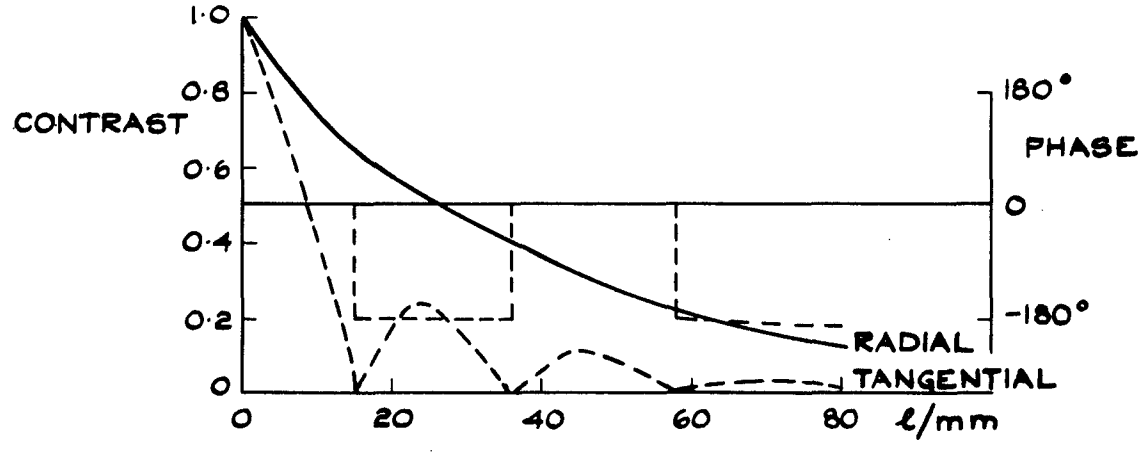

(b) 12° OFF-AXIS

FIG. 16 (a & b) TYPICAL RESULTS
(24" F/5·6 LENS: λ = 5876 Å)

Marchant, A. C.
Lello, Margaret

535.316/317

CALCULATION OF OPTICAL TRANSFER FUNCTIONS FROM LENS DESIGN DATA

Royal Aircraft Establishment Technical Report 65031 February 1965

This Report describes the basic theory and the method of operation of a computer programme developed at Imperial College, London, for calculating the optical transfer function of a lens system. The programme determines the wavefront aberration, and the shape of the exit pupil (vignetted or otherwise) and uses this information to derive the transfer function in any image plane and at any field angle. Typical results, for a modern aerial reconnaissance lens, are given and compared with measurement.

Marchant, A. C.
Lello, Margaret

535.316/317

CALCULATION OF OPTICAL TRANSFER FUNCTIONS FROM LENS DESIGN DATA

Royal Aircraft Establishment Technical Report 65031 February 1965

This Report describes the basic theory and the method of operation of a computer programme developed at Imperial College, London, for calculating the optical transfer function of a lens system. The programme determines the wavefront aberration, and the shape of the exit pupil (vignetted or otherwise) and uses this information to derive the transfer function in any image plane and at any field angle. Typical results, for a modern aerial reconnaissance lens, are given and compared with measurement.

Marchant, A. C.
Lello, Margaret

535.316/317

CALCULATION OF OPTICAL TRANSFER FUNCTIONS FROM LENS DESIGN DATA

Royal Aircraft Establishment Technical Report 65031 February 1965

This Report describes the basic theory and the method of operation of a computer programme developed at Imperial College, London, for calculating the optical transfer function of a lens system. The programme determines the wavefront aberration, and the shape of the exit pupil (vignetted or otherwise) and uses this information to derive the transfer function in any image plane and at any field angle. Typical results, for a modern aerial reconnaissance lens, are given and compared with measurement.

Marchant, A. C.
Lello, Margaret

535.316/317

CALCULATION OF OPTICAL TRANSFER FUNCTIONS FROM LENS DESIGN DATA

Royal Aircraft Establishment Technical Report 65031 February 1965

This Report describes the basic theory and the method of operation of a computer programme developed at Imperial College, London, for calculating the optical transfer function of a lens system. The programme determines the wavefront aberration, and the shape of the exit pupil (vignetted or otherwise) and uses this information to derive the transfer function in any image plane and at any field angle. Typical results, for a modern aerial reconnaissance lens, are given and compared with measurement.

DETACHABLE ABSTRACT CARDS